

Diphenylpyrazoles as Replication Protein A inhibitors

Alex G. Waterson, J. Phillip Kennedy, James D Patrone, Nicholas F. Pelz,
Michael D Feldkamp, Andreas O. Frank, Bhavatarini Vangamudi, Elaine Maria
Souza-Fagundes, Olivia W. Rossanese, Walter J Chazin, and Stephen W. Fesik

ACS Med. Chem. Lett., **Just Accepted Manuscript** • DOI: 10.1021/ml5003629 • Publication Date (Web): 11 Nov 2014

Downloaded from <http://pubs.acs.org> on November 14, 2014

Just Accepted

“Just Accepted” manuscripts have been peer-reviewed and accepted for publication. They are posted online prior to technical editing, formatting for publication and author proofing. The American Chemical Society provides “Just Accepted” as a free service to the research community to expedite the dissemination of scientific material as soon as possible after acceptance. “Just Accepted” manuscripts appear in full in PDF format accompanied by an HTML abstract. “Just Accepted” manuscripts have been fully peer reviewed, but should not be considered the official version of record. They are accessible to all readers and citable by the Digital Object Identifier (DOI®). “Just Accepted” is an optional service offered to authors. Therefore, the “Just Accepted” Web site may not include all articles that will be published in the journal. After a manuscript is technically edited and formatted, it will be removed from the “Just Accepted” Web site and published as an ASAP article. Note that technical editing may introduce minor changes to the manuscript text and/or graphics which could affect content, and all legal disclaimers and ethical guidelines that apply to the journal pertain. ACS cannot be held responsible for errors or consequences arising from the use of information contained in these “Just Accepted” manuscripts.

Diphenylpyrazoles as Replication Protein A inhibitors

Alex G. Waterson^{2,3}, J. Phillip Kennedy^{1†}, James D. Patrone¹, Nicholas F. Pelz¹, Michael D. Feldkamp¹, Andreas O. Frank^{1†}, Bhavatarini Vangamudi^{1†}, Elaine M. Souza-Fagundes^{1†}, Olivia W. Rossanese¹, Walter J. Chazin^{1,3}, Stephen W. Fesik^{1,2,3*}

¹Department of Biochemistry, ²Department of Pharmacology Vanderbilt University School of Medicine, ³Department of Chemistry, Vanderbilt University, Nashville, TN 37232 (USA)

KEYWORDS: Replication protein A, fragment-based discovery, medicinal chemistry

ABSTRACT: Replication Protein A is the primary eukaryotic ssDNA binding protein that has a central role in initiating the cellular response to DNA damage. RPA recruits multiple proteins to sites of DNA damage via the N-terminal domain of the 70 kDa subunit (RPA70N). Here we describe the optimization of a diphenylpyrazole carboxylic acid series of inhibitors of these RPA-protein interactions. We evaluated substituents on the aromatic rings as well as the type and geometry of the linkers used to combine fragments, ultimately leading to sub-micromolar inhibitors of RPA70N protein-protein interactions.

Replication Protein A (RPA), the eukaryotic ssDNA binding protein, is a widely used scaffold for DNA transactions that functions by protecting and organizing ssDNA, as well as recruiting other proteins of the DNA processing machinery.^{1,2} RPA is a heterotrimer; the 70-kDa subunit contains an OB-fold at its N-terminus, RPA70N, that serves as a protein recruitment module.¹⁻³ In particular, this domain plays a crucial role in recruiting DNA damage response and repair proteins to sites of DNA damage, using a conserved motif that interacts with a basic cleft at the surface of RPA70N.⁴⁻⁶

Based on the critical role of the RPA70N interactions with target proteins in initiating DNA damage response, inhibition of these interactions has the potential to suppress damage response pathways and may represent a promising point of intervention for cancer therapy. A selective inhibitor of the RPA70N-protein interactions that does not abrogate ssDNA binding or important scaffolding activities of the entire protein would provide a powerful tool for focused exploration of the role of RPA in checkpoint signaling and enable studies to confirm the therapeutic potential of RPA70N inhibition, as well as a potential starting point for new cancer drugs. Indeed, a recent report describes a small molecule that binds to RPA70N and demonstrates activity in a xenograft tumor model.⁷

Toward the discovery of new inhibitors, we have reported the use of a fragment-based screen to identify small molecules that bind to the basic cleft of RPA70N, the elaboration of these fragments to produce two triazole series (**1**, **2**), and preliminary linking efforts to obtain molecules (e.g. **3**) that span the entire cleft (Figure 1).^{8,9} Here, we describe the optimization of the linked compounds, including the details of the structure-activity relationships (SAR) for binding to RPA70N and the physicochemical properties of selected compounds.

The synthetic route used to produce linked compounds such as **3**⁸ was adapted to explore the SAR of the diphenylpyrazoles and linked compounds described herein. The basic route in-

volves a cyclodehydration reaction to generate functionalized diphenylpyrazoles that are elaborated in various ways to construct the inhibitor compounds. Full details of the compound syntheses are reported in the supplementary information.

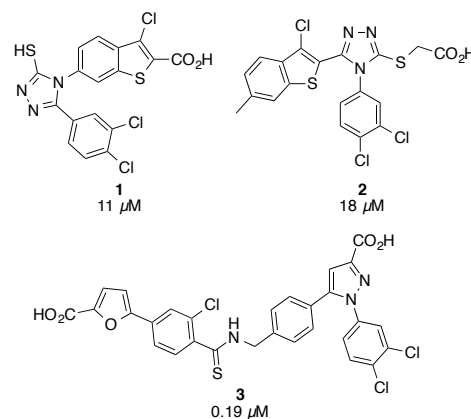
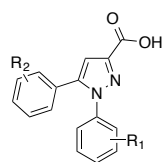


Figure 1. Our previously reported RPA70N inhibitors.^{8,9} Values represent binding affinities determined in an FPA assay.

We explored the SAR of the 1,5-diphenyl pyrazoles via an organized system of chemical synthesis and targeted purchasing (Table 1). The initial analogs were evaluated for binding to RPA70N using HSQC NMR-based titrations. Of note, the carboxylic acid was critical for binding, as all analogs devoid of this acid, or with ester or amide derivatives, displayed sharply reduced binding affinity to the protein (not shown).

We quickly established a preference for 3- and 4- position substituents on this ring (compare **4a** versus **4c,d**). The most robust trend evident in this initial group was a very strong preference for halogens in the 3- and 4-positions of the 1-phenyl ring (e.g. **4f**). Indeed, we found a distinct binding affinity advantage for a 3,4-dichlorophenyl substitution, mirroring the preference found in a prior series of RPA70N binding

Table 1. Pyrazole SAR in Site-1.



Cpd	R ₁	R ₂	NMR K _d (μM) ^a	K _d (μM) ^b	% inh ^c	LE ^d
4a	-H	-H	1150			0.21
4b	4-OMe	-H	895	>500	18	0.19
4c	3-Me	-H	580	>500		0.22
4d	4-Cl	4-Cl	260	>500	24	0.23
4e	2,4-diCl	4-Cl	410	>500	29	0.21
4f	3,4-diCl	4-Cl	54	67 ± 9		0.25
4g	3-Me	4-OMe		>500	20	N/A
4h	4-Me	4-OMe		>500	15	N/A
4i	3-Br	4-OMe		140 ± 2.8		0.23
4j	4-Br	4-OMe		>500	24	N/A
4k	3-Cl	4-OMe		>500	35	N/A
4l	4-Cl	4-OMe		>500	19	N/A
4m	3,4-diCl	4-OMe		79 ± 1.4		0.24
4n	cyclohexyl ^e	4-OMe		>500	9	N/A

^aK_d values determined from 6 point NMR titrations. ^bAverage K_d values (n=2) calculated using Cheng-Prusoff equation from IC₅₀ values measured in FPA competition assay. ^cAmount of displacement of labeled probe at the highest compound concentration used, 500 μM. ^dLE = ligand efficiency. Values calculated using LE = 1.4 * pK_d/HAC, using FPA data if available, NMR data if the FPA data did not give a K_d value. ^eRepresents replacement of the entire phenyl ring.

compounds and in a potent stapled helix peptide inhibitor of RPA70N.^{9,10} It is likely that the halogen substituents lead to additional hydrophobic interactions and a possible halogen bond in the lipophilic cavity near Ser55 in RPA70N (Site-1) in which the N-phenyl ring of the pyrazole compounds bind.⁸

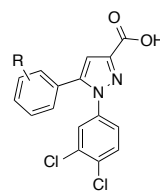
Compound **4f** displayed sufficient NMR-derived binding affinity to also be evaluated in an FPA competition assay,¹¹ which produced a comparable binding affinity of 67 μM. This assay was used exclusively to profile later analogs. To identify additional substituents that might effectively fill Site-1, we initiated a more thorough investigation of the 1-phenyl ring SAR, systematically exploring lipophilic and halogen substitutions at the 3- and 4- positions, using a 4-methoxyphenyl ring at the pyrazole 1-position as a standard substitution. Unfortunately, most of these analogs displayed a loss of binding affinity 10-fold or greater compared with **4f**, with only the 3-Br analog **4i** producing a full concentration-response curve. Some rank ordering of the compounds was determined by examining the maximal displacement of the FPA probe at the highest compound concentration. From this, it was generally evident that 3-position substitutions were favored over 4-position substitutions and that a bromide was favored over chloro and me-

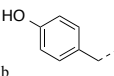
thyl at the 3-position. Larger substitutions in either the 3- or 4-position, for example, the use of bicyclic ring systems and larger alkyl groups such as isopropyl, were completely ineffectual (data not shown). However, as observed with **4f**, combining the 3- and 4-chloro substitutions produces a large gain in binding affinity (**4m**). Finally, we established an advantage for a phenyl substituent on the 1- position of the pyrazole (compare **4n** versus **4a**).

Holding the 3,4-dichlorophenyl substitution pattern constant, we initiated an investigation of 5-phenyl ring modifications. In general, a relatively wide range of substitutions was tolerated with minimal changes in binding affinity or ligand efficiency (LE) (Table 2). We observed a slight preference for 4-position substitutions over 3-position analogs (**5b** vs. **5c**, **5d** vs. **5e**). A 4-cyano substituent was 4-fold less potent than the methyl analog (**5b** v. **5f**) and the corresponding amine-containing **5g** was completely inactive. While some polar groups were tolerated in this region (e.g. **5d**, **5e**, **5h**, and **5i**), heterocyclic ring systems were generally disfavored (e.g. **5j**). In addition, a methylene could not be introduced between the pyrazole and the phenyl ring without a substantial loss of binding affinity (e.g. **5k**).

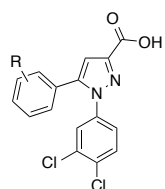
Many SAR trends in this series can be rationalized by the co-crystal structures of the molecules bound to the basic cleft of RPA70N. As previously described,⁸ 1,5-diarylpyrazoles bind

Table 2. Pyrazole 5-position SAR.



Cpd	R	K _d (μM) ^a	LE ^c
4f	4-Cl	67 ± 9	0.25
5a	H	123 ± 4.2	0.25
5b	3-Me	90 ± 1.4	0.25
5c	4-Me	72 ± 4.9	0.25
5d	3-CO ₂ H	129 ± 17	0.22
5e	4-CO ₂ H	59 ± 3.5	0.24
5f	4-CN	310 ± 21	0.20
5g	4-CH ₂ NH ₂	>500	N/A
5h	4-NH ₂	227 ± 27	0.22
5i	4-OH	104 ± 15	0.24
5j	4-(2-furanyl) ^b	>500	N/A
5k		>500	N/A

^aAverage K_d values (n=2) calculated using Cheng-Prusoff equation from IC₅₀ values measured in FPA competition assay. ^bEntire ring system replaces the phenyl. ^cLE = ligand efficiency. Values values calculated using LE = 1.4 * pK_d/HAC, using the FPA data.

Table 3. Extension of the diphenylpyrazoles.

Cpd	R	K _d (μM) ^a	LE ^b
4f	4-Cl	67 ± 9	0.25
6a	4-CONHCH ₂ (phenyl)	83 ± 18	0.18
6b	4-CONHCH ₂ (4-methoxyphenyl)	45 ± 11	0.18
6c	4-CH ₂ NHCO(phenyl)	90 ± 15	0.18
6d	4-CH ₂ NHCO(4-methoxyphenyl)	72 ± 7.8	0.17
6e	4-CH ₂ NHCO(4-bromophenyl)	35 ± 2.1	0.19
6f	4-CSNHCH ₂ (phenyl)	18 ± 6.4	0.21
6g	4-CSNHCH ₂ (4-methoxyphenyl)	23 ± 4.2	0.19
6h	4-CH ₂ NHCS(4-bromophenyl)	15 ± 1.4	0.20
6i	4-CH ₂ NHSO ₂ (phenyl)	70 ± 9.2	0.17
6j	4-CH ₂ NHSO ₂ (4-trifluoromethoxyphenyl)	56 ± 2.8	0.16

^aAverage K_d values (n=2) calculated using Cheng-Prusoff equation from IC₅₀ values measured in FPA. ^bLE = ligand efficiency. Values calculated using LE = 1.4 * pK_d / HAC, using the FPA data.

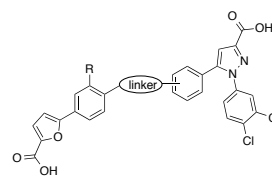
with good affinity to Site-1 and are located above Ser55 in the protein. The 3,4-dichloro substitution more effectively fills the Site-1 pocket compared with other substitution patterns. Interestingly, the 4-position chloride is located 3.5-3.8 Å away from the sidechain oxygen of Ser 55, at bond angles of 150-160°, indicating a possible halogen bond interaction. In addition, the 5-position phenyl ring is located such that substitutions at the 3- and 4-positions are aimed directly down the basic cleft. Thus, it is reasonable to expect that a range of modifications would be tolerated on this ring. The hydrophobic nature of the central portion of the cleft may also explain the poor binding affinity of the basic amine-containing **5g**.

Because the 5-phenyl ring is ideally positioned in the cleft of RPA70N to tolerate larger functionality, we elected to employ a fragment growing strategy to seek affinity improvements. Using the carboxylic acid of **5e** and the amine of **5g** as synthetic handles, we synthesized an exploratory series of substituted amides, thioamides, and sulfonamides with phenyl moieties predicted to extend down the cleft of RPA70N (Table 3). Most of the amide and sulfonamide analogs failed to demonstrate substantial improvement over **4f** or **5e**. In general, the best analogs within this group (**6e-h**) employ highly lipophilic thioamide-containing substitutions and display binding affinities 2-3 fold better than **4f**. As these substitutions did not add significant affinity to the molecules to offset large increases in molecular weight, the corresponding ligand efficiencies are lower. However, it should be noted that the thioamides had generally higher ligand efficiencies than their amide counter-

parts, indicating the likelihood of a specific interaction. Interestingly, several attempts to replace the appended phenyl rings with heterocycles produced compounds with extremely weak binding to the protein (data not shown), reinforcing the preference for lipophilic substitutions in this region of the protein.

Fragment linking to generate high affinity inhibitors is considered difficult to achieve, due to the specific geometrical constraints that must be precisely matched to successfully link two molecules that bind to adjacent sites in a protein. However, several successful examples demonstrate the power of this approach.¹² RPA70N appeared ideally suited for this strategy, as a single fragment screen identified multiple series of fragments that bind to two different, nearby sites in the protein.

An ether linker should provide flexibility and allow a linked compound to achieve a binding pose similar to the original fragments. However, connecting the optimized diphenylpyrazole and a furan-based fragment with either a two atom link⁸ or a longer, PEG-inspired 4 atom link (data not shown) proved less successful than anticipated. **We virtually docked**

Table 4. Fragment linking and optimization.

Cpd	R	Linker	Linker position	K _d (μM) ^a	LE ^b
7a	H		para	57 ± 1.4	0.15
7b	H		para	8.2 ± 2.6	0.17
7c	H		meta	22 ± 4.2	0.16
7d			para	2.5 ± 0.1	0.20
7e	H		para	1.5 ± 0.3	0.20
7f	H		para	0.55 ± 0.1	0.22
7g	Cl		para	9.4 ± 3.8	0.17
7h	Cl		para	0.48 ± 0.1	0.22
7i ⁸	Cl		para	2.9 ± 0.8	0.18
3 ⁸	Cl		para	0.19 ± 0.03	0.23
7j	-		para	0.54 ± 0.2	0.21

^aAverage K_d values (n=2) calculated using Cheng-Prusoff equation from IC₅₀ values measured in FPA. ^bLE = ligand efficiency. Values calculated using LE = 1.4 * pK_d / HAC, using the FPA data. ^cn=1 data. ^dThe linker is attached to the meta position of the furan phenyl ring and the para position of the pyrazole phenyl ring.

prospective molecules into RPA70N using the Induced Fit Docking Protocol available from Schrodinger.¹³ This suggested exploration of three atom linkers. Thus, we used the amine of **5g** as a synthetic handle (Table 4). The initial compound, **7a**, reinforced the lack of tolerance for a charged atom in this region of the protein. Acetylating this amine produced a 10-fold gain in binding affinity (**7b**). However, the binding mode of the compound in complex with RPA70N reveals a linker conformation that is kinked to accommodate the requirements of the original fragment molecules in Site-1 and Site-2 (Figure 2A).

Further molecular modeling also suggested that an sp^2 hybridized carbon in the linker would improve the binding geometry. This idea was explored in the context of both meta- and para-linked compounds, with a carbonyl or thiocarbonyl attached to the 5-phenyl ring of the pyrazole. In accordance with the computational predictions, linkers with an sp^2 center were generally superior to those with saturated linkers. We found a distinct preference for a more lipophilic thioamide substitution over the amide (**7c** vs. **7e**, **7g** vs. **7h**). The thioamide appears to occupy a small hydrophobic space under Leu87 (Figure 2B), potentially explaining the enhanced binding affinity granted by this substitution. Placing the linker on the 3-position of the furan phenyl ring offered no significant advantage over the 4-position (**7d** vs. **7e**). In addition, placement of the thioamide carbonyl on the furan phenyl ring was found to be superior to placement on the 5-phenyl pyrazole (**7f** vs. **7e**). The structure of **7f** in complex with RPA70N reveals that the sulfur is able to access the Leu87 pocket with less contortion of the linker portion of the molecule (blue circle, Figure 2C), leading to a compound with submicromolar binding affinity to RPA70N.

Introduction of a 3-position chloride (inspired by the fragment SAR)⁸ on the phenylfuran produced affinity gains over the des-chloro variants (e.g. **7h** vs. **7e**, **3** vs. **7f**), probably due to

the occupation of space in the binding site above Met57 (Figure 2D). The application of all of these strategies produced compounds with the highest binding affinity to RPA70N and with ligand efficiencies similar to the original pyrazole-containing compounds (**3**).⁸ A cyclic thioamide linker (**7j**) also places non-polar atoms under Leu87, occupies the space above Met57 (Figure 2E), and binds with submicromolar affinity.

We explored removal or replacement of one or both of the two carboxylic acids from the high affinity linked compounds to guard against possible issues with poor cellular permeability. Indeed, we assessed the permeability of compound **3** in the Caco-2 cell line and found that it possesses poor intrinsic permeability of $<0.21 \times 10^{-6}$ cm/s and is subject to significant pgp-mediated efflux (efflux ratio >32). Applying the optimal thioamide positioning, we explored isosteres of the 2-furan carboxylic acid designed to maintain the key binding interactions with Arg31 (**8-10**, Figure 3). The best of these compounds (**9**) displays low micromolar binding affinity. We also explored the removal of the pyrazole carboxylic acid. Compound **11**, devoid of this carboxylic acid, has a 1.7 μ M binding affinity to RPA70N in our FPA assay and an intrinsic permeability of 14.5×10^{-6} cm/s, with no pgp efflux noted. The X-ray co-crystal structure of this molecule, overlaid with the previously reported structure of **7j** (Figure 2F), demonstrates that the lack of interaction with Arg31 leads to a slight relaxation of the molecule in the pocket and a slight shift toward Site-2. This shift, and the missing interaction with Arg31, may explain the 10-fold loss in binding affinity compared with **3**.

Discussion/Conclusions: Interactions mediated by the RPA70N domain of RPA are essential for recruiting a number of key proteins to initiate DNA damage response and repair (e.g. ATRIP, MRE11, RAD9). Each of these interactions is

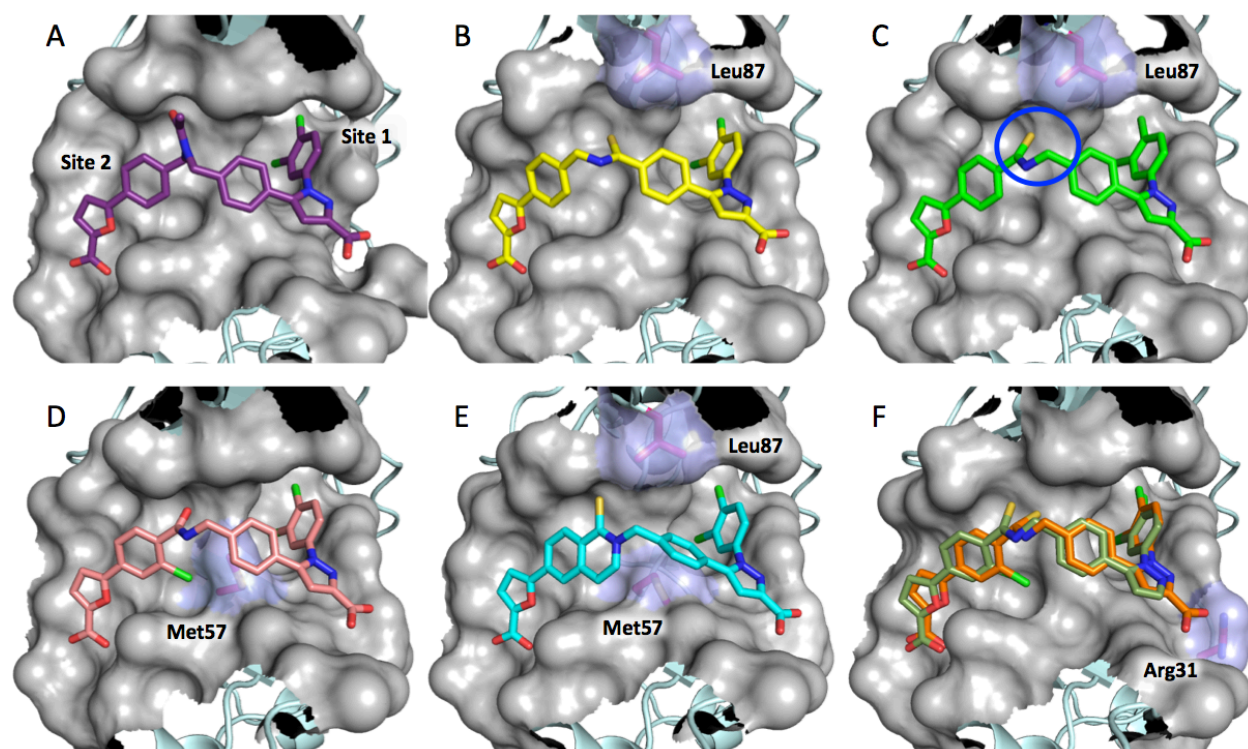
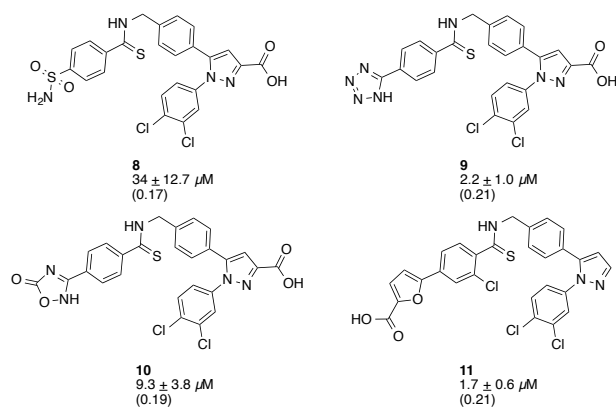


Figure 2. X-ray co-crystal structures of compounds in complex with RPA70N. **A)** Compound **7b** (PDB 4R4Q), **B)** Compound **7e** (4R4O), **C)** Compound **7f** (4R4T), **D)** Compound **7i** (4R4C), **E)** Compound **7j** (4R4I), **F)** Compound **11** (green, 4LWC) overlaid with **3** (orange).

Figure 3. Linked compounds with acid replacements.^a

^aAverage K_d values (n=2) calculated using Cheng-Prusoff equation from IC_{50} values measured in FPA. Ligand efficiency (LE) values in parentheses.

mediated by the binding of RPA70N to an amphiphilic helix from the target protein. The amphiphilic nature of the RPA70N binding site seems to produce strict requirements for a tightly binding compound, as evidenced by our optimization efforts. A significant amount of hydrophobic contact area must be engaged, and the binding must be anchored by interaction with charged residues at the outer edges of the cleft.

We have generated molecules with sub-micromolar binding affinity to this cleft using fragment linking and subsequent optimization. The requirements to successfully bind to the basic cleft of RPA70N result in small molecules with relatively poor pharmaceutical properties. Careful molecular design to remove one of the negatively charged groups, yet maintain the other important contributors to binding affinity, has produced a compound with enhanced permeability. However, this trade-off results in loss of binding affinity to the protein, pointing toward opportunities for future optimization. The molecules described here represent a useful starting point for obtaining potent and cell permeable RPA inhibitors that could be used as tools to validate that inhibition of the RPA70N-protein interactions is a therapeutically relevant avenue for suppression of the DNA damage response as an adjuvant cancer treatment.

ASSOCIATED CONTENT

Supporting Information

Synthetic procedures, compound characterization, and assay protocols. This material is available free of charge via the Internet at <http://pubs.acs.org>. The atomic coordinates and structure factors for the X-ray crystal structures of RPA70N in complex with compounds **7b** (4R4Q), **7e** (4R4O), **7f** (4R4T), **7i** (4R4C), **7j** (4R4I), and **11** (4LWC) have been deposited in the Protein Data Bank RCSB PDB.

AUTHOR INFORMATION

Corresponding Author

* Tel: 615-322-6303. E-mail: stephen.fesik@vanderbilt.edu.

Present Addresses

†(J.P.K.) Revance Therapeutics, Newark, CA 94560, United States; (A.O.F.) Novartis Institutes for BioMedical Research (NIBR), Global Discovery Chemistry, Emeryville, California 94608, United States; (B.V.) UT MD Anderson Cancer Center,

Houston, TX, 77054; (E.M.S.-F.) Federal University of Minas Gerais, Belo Horizonte, Brazil.

Funding Sources

Funding of this research was provided in part by NIH grants 5DP1OD006933/8DP1CA174419 (NIH Director's Pioneer Award) and R01CA174887 to S.W.F., R01GM065484 and P01CA092584 to W.J.C., ARRA stimulus grant (5RC2CA148375) to Lawrence J. Marnett, F32ES021690 to M.D.F., F32CA174315 to J.D.P. and 5T21CA9582-24 to Scott Hiebert (Trainee: J.P.K.). A.O.F. was supported by the Deutscher Akademischer Austausch Dienst (DAAD) postdoctoral fellowship and E.M.S.-F. was supported by fellowship from the National Council for Scientific and Technological Development – CNPq and Federal University of Minas Gerais/Brazil. The NMR instrumentation used in this work was supported by NIH grant S10 RR025677-01 and by NSF grant DBI-0922862.

ACKNOWLEDGMENT

We would like to thank Dr. David Cortez for his intellectual contributions in the conception of this project.

REFERENCES

- (1) Wold, M. S. Replication protein A: A heterotrimeric, single-stranded DNA-binding protein required for eukaryotic DNA metabolism. *Annu. Rev. Biochem.* **1997**, *66*, 61-92.
- (2) Wold, M. S.; Kelly, T. Purification and Characterization of Replication Protein-a, a Cellular Protein Required for Invitro Replication of Simian Virus-40 DNA. *Proc. Natl. Acad. Sci. U.S.A.* **1988**, *85*, 2523-2527.
- (3) Xu, X.; Vaithiyalingam, S.; Glick, G. G.; Mordes, D. A.; Chazin, W. J.; Cortez, D. The Basic Cleft of RPA70N Binds Multiple Checkpoint Proteins, Including RAD9, To Regulate ATR Signaling. *Mol. Cell Biol.* **2008**, *28*, 7345-7353.
- (4) Fanning, E.; Klimovich, V.; Nager, A. R. A dynamic model for replication protein A (RPA) function in DNA processing pathways. *Nucleic Acids Res.* **2006**, *34*, 4126-4137.
- (5) Cortez, D.; Guntuku, S.; Qin, J.; Elledge, S. J. ATR and ATRIP: Partners in checkpoint signaling. *Science* **2001**, *294*, 1713-1716.
- (6) Cimprich, K. A.; Cortez, D. ATR: an essential regulator of genome integrity. *Nature Rev. Mol. Cell Biol.* **2008**, *9*, 616-627.
- (7) Glanzer, J. G.; Liu, S.; Wang, L.; Mosel, A.; Peng, A.; Oakley, G. G. *Cancer Res.* **2014**, *74*, 5165-5172.
- (8) Frank, A. O.; Feldkamp, M. D.; Kennedy, J. P.; Waterson, A. G.; Pelz, N. F.; Patrone, J. D.; Vangamudi, B.; Camper, D. V.; Rossanese, O. W.; Chazin, W. J.; Fesik, S. W. Discovery of a potent inhibitor of replication protein a protein-protein interactions using a fragment-linking approach. *J. Med. Chem.* **2013**, *56*, 9242-9250.
- (9) Patrone, J. D.; Kennedy, J. P.; Frank, A. O.; Feldkamp, M. D.; Vangamudi, B.; Pelz, N. F.; Rossanese, O. W.; Waterson, A. G.; Chazin, W. J.; Fesik, S. W. Discovery of Protein-Protein Interaction Inhibitors of Replication Protein A. *ACS Med. Chem. Lett.* **2013**, *4*, 601-605.
- (10) Frank, A. O.; Vangamudi, B.; Feldkamp, M. D.; Souza-Fagundes, E. M.; Luzwick, J. W.; Cortez, D.; Olejniczak, E. T.; Waterson, A. G.; Rossanese, O. W.; Chazin, W. J.; Fesik, S. W. Discovery of a potent stapled helix peptide that binds to the 70N domain of replication protein A. *J. Med. Chem.* **2014**, *57*, 2455-2461.
- (11) Souza-Fagundes, E. M.; Frank, A. O.; Feldkamp, M. D.; Dorset, D. C.; Chazin, W. J.; Rossanese, O. W.; Olejniczak, E. T.; Fesik, S. W. A high-throughput fluorescence polarization anisotropy assay for the 70N domain of replication protein A. *Anal. Biochem.* **2012**, *421*, 742-749.
- (12) Ichihara, O.; Barker, J.; Law, R. J.; Whittaker, M. Compound Design by Fragment-Linking. *Mol. Inform.* **2011**, *30*, 298-306.
- (13) Schrödinger Suite 2009 Induced Fit Docking protocol; Glide version 5.5, Schrödinger, LLC, New York, NY, 2009; Prime version 2.1, Schrödinger, LLC, New York, NY, 2009.

SYNOPSIS TOC

Diphenylpyrazoles as Replication Protein A inhibitors

Alex G. Waterson^{2,3}, J. Phillip Kennedy^{1†}, James D. Patrone¹, Nicholas F. Pelz¹, Michael D. Feldkamp¹,
Andreas O. Frank^{1†}, Bhavatarini Vangamudi^{1†}, Elaine M. Souza-Fagundes^{1†}, Olivia W. Rossanese¹,
Walter J. Chazin^{1,3}, Stephen W. Fesik^{1,2,3*}

